

RESEARCH

Open Access



A lipid metabolism-related gene signature reveals dynamic immune infiltration of the colorectal adenoma-carcinoma sequence

Jie Chen^{1,3†}, Jianfang Ye^{2,3†} and Renxu Lai^{1,3*}

Abstract

Background Lipid metabolism-related genes (LMRGs) have been reported to be correlated with the immune infiltration of colorectal cancer (CRC). This study aimed to investigate the immune infiltration characteristics along the colorectal adenoma-carcinoma sequence (ACS) based on LMRGs.

Methods Gene expression data of colorectal adenoma and carcinoma samples were obtained from the public databases. The “limma” package was applied to determine the differentially expressed LMRGs. Unsupervised consensus clustering was used to cluster colorectal samples. The features of the tumor microenvironment were analyzed by the “ESTIMATE”, “GSVA”, and “TIDE” algorithms.

Results The expression of 149 differentially expressed LMRGs was defined as the LMRG signature. Based on this signature, the adenoma and carcinoma samples were divided into three clusters. Unexpectedly, these sequential clusters showed a directional relationship and collectively constituted the progressive course of colorectal ACS. Interestingly, the LMRG signature revealed that adenoma progression was accompanied by a progressive loss of immune infiltration and a stepwise establishment of a cold microenvironment, but carcinoma progression was characterized by a progressive gain of immune infiltration and a gradual establishment of a hot microenvironment.

Conclusions The LMRG signature reveals dynamic immune infiltration along the colorectal ACS, which substantially changes the understanding of the tumor microenvironment of CRC carcinogenesis and provides novel insight into the role of lipid metabolism in this process.

Keywords Colorectal cancer, Adenoma-carcinoma sequence, Lipid metabolism, Immune infiltration, Tumor microenvironment

[†]Jie Chen and Jianfang Ye contributed equally.

*Correspondence:

Renxu Lai

lairenxu@mail.sysu.edu.cn

¹Department of Gastroenterology, The Fifth Affiliated Hospital of Sun Yat-sen University, Zhuhai, Guangdong Province, China

²Department of Endocrinology and Metabolism, The Fifth Affiliated Hospital of Sun Yat-sen University, Zhuhai, Guangdong Province, China

³Molecular Imaging Center, the Fifth Affiliated Hospital of Sun Yat-sen University, Zhuhai, Guangdong Province, China



Introduction

In 2020, global cancer statistics reported 1.8 million new cases and 880,800 deaths due to colorectal cancer (CRC) [1]. Most cases of CRC are sporadic, accounting for over 80% of all diagnoses [2]. There is an established model of sporadic CRC known as the adenoma-carcinoma sequence (ACS), which describes the progressive process from normal mucosa to adenoma to carcinoma and is responsible for 85–90% of sporadic CRC cases [3].

CRC risk is predominantly driven by environmental factors, particularly a high-fat diet. Dysregulation in lipid metabolism has been found to be the most prominent metabolic alteration in cancer. Abnormal lipid metabolism can promote tumor growth and progression by modulating ferroptosis-induced cell death, promoting metastasis, and interacting with the tumor microenvironment [4, 5]. Moreover, activating oncogenes drive abnormal lipid metabolism to provide cancer cells with energy, lipid components, and signaling molecules that are needed for proliferation, invasion, and metastasis [4]. In particular, a high-fat diet is a highly relevant risk factor in CRC and is associated with nearly 80% of CRC cases [6]. Regardless of the formation and cancerous transformation of adenomas or the progression and metastasis of CRC, a high-fat diet is an important promoting factor [7, 8]. Therefore, understanding the role of abnormal lipid metabolism in CRC carcinogenesis is of great interest.

Tumor heterogeneity is a significant characteristic of cancers and a great challenge in the oncology field. Tumor heterogeneity shapes the tumor microenvironment and plays decisive roles in tumor initiation, progression, and drug resistance [9]. Several studies have provided novel insight into lipid metabolic heterogeneity in CRC based on lipid metabolism-related genes (LMRGs) and reported that the LMRGs were associated with immune infiltration and were useful for predicting the prognosis of CRC patients [10–12]. However, no study has focused on the role of LMRGs in the complete

course of the colorectal ACS. In particular, the relationship between LMRGs and immune infiltration along the colorectal ACS is unclear. This study aimed to investigate the immune infiltration characteristics along the ACS based on LMRGs.

Methods

Data collection and preparation

The gene expression datasets GSE41657 (12 normal, 51 adenoma, and 25 carcinoma samples), GSE37364 (38 normal, 29 adenoma, and 27 carcinoma samples), and GSE117606 (65 normal, 69 adenoma, and 74 carcinoma samples) were obtained from the Gene Expression Omnibus (GEO) repository, and RNA sequencing data of patients with colon adenocarcinoma (COAD, n=429) were downloaded from The Cancer Genome Atlas (TCGA) database.

A total of 776 human LMRGs were obtained from 7 gene sets in the Molecular Signature Database (<http://gsea-msigdb.org>) (Table 1) [13]. As a supplement, 833 LMRGs were preliminarily obtained by taking the union of the above 776 LMRGs and the LMRGs reported by Sun X et al. [14]. However, only 711 genes were used for differential expression analyses because not all the LMRGs could be detected during sequencing (Sheet 1).

Differentially expressed LMRG analyses and pathway enrichment analyses

The GSE41657 and GSE37364 datasets were adopted to screen the differentially expressed LMRGs among normal mucosa, colorectal adenoma, and colorectal carcinoma. Each dataset was analyzed independently, and the differentially expressed LMRGs were taken from their intersection. Principal component analysis was used to identify potential outliers in each dataset. The “limma” package [15] was used to determine the differentially expressed LMRGs with adjusted *P* values less than 0.05 and absolute value of fold change more than 1.5 as the threshold. Kyoto Encyclopedia of Genes and Genomes (KEGG) and Gene Ontology (GO) analyses were used to elucidate the function of differentially expressed LMRGs by the “clusterProfiler” package [16].

Unsupervised consensus clustering analyses

Unsupervised consensus clustering is a popular method to identify robust clusters and has been extensively utilized in analyzing omics data [17–19]. The “ConsensusClusterPlus” package [20] was used to apply unsupervised consensus clustering to facilitate the classification of colorectal tumors based on the transcriptome of differentially expressed LMRGs, and repeated subsampling was set 500 times to ensure reliability. For the convenience of analysis, the colorectal adenoma and carcinoma samples were divided into three clusters based

Table 1 Retrieving the genes related to lipid metabolism

ID	Gene set	Database	Gene count
M699	FATTY ACID METABOLISM	KEGG	42
M15902	GLYCEROLIPID METABOLISM	KEGG	49
M27854	FATTY ACID METABOLISM	REACTOME	177
M14690	MITOCHONDRIAL FATTY ACID BETA OXIDATION	REACTOME	37
M706	GLYCEROPHOSPHOLIPID BIOSYNTHESIS	REACTOME	161
M27451	METABOLISM OF LIPIDS	REACTOME	742
M649	PHOSPHOLIPID METABOLISM	REACTOME	212
Not applicable	LMRGs reported by Sun X, et al. (doi: https://doi.org/10.1155/2022/3170950)	Pubmed	776
Unique			833

on the consensus clustering algorithm (adenoma: A1, A2, and A3; carcinoma: C1, C2, and C3). The t-distributed stochastic neighbor embedding (t-SNE) was applied to determine the difference in each cluster by the “Rtsne” package [21] based on the expression of differentially expressed LMRGs.

Evaluation of the tumor microenvironment

The stromal, immune, and ESTIMATE scores were calculated for each sample using the ESTIMATE algorithm [22]. The stromal score and immune score positively correlate with the matrix and immune in the tumor microenvironment, and the ESTIMATE score positively correlates with tumor purity. Gene set variation analyses were used to quantify the immune cells according to the 28 immune cell gene sets retrieved from a previous study [23] by the “GSVA” package. The Tumor Immune Dysfunction and Exclusion (TIDE) algorithm was used to calculate the antitumor immunotherapeutic response [24], which includes the dysfunction score of T lymphocytes, exclusion score of T lymphocytes, and dysfunction and exclusion of T lymphocytes (TIDE score). A higher dysfunction score, exclusion score, and TIDE score indicate a higher likelihood of antitumor immune dysfunction or escape.

Statistical analysis

Statistical analyses were performed with R software (version 4.2.2). Kaplan–Meier (K–M) survival analyses were performed with the “survival” and “survminer” packages. The log-rank test was used to estimate the differences among K–M survival curves. Sankey plots were generated with the “ggalluvial” package [25]. Differences of continuous variables were calculated using a t test or analysis of covariance. All statistical tests were two-sided, and a *P* value less than 0.05 was considered significant.

Results

Identification of differentially expressed LMRGs

The GSE41657 and GSE37364 datasets were used to identify the differentially expressed LMRGs. Six overlapping upregulated and 22 overlapping downregulated LMRGs in the colorectal adenoma compared with the normal mucosa (Fig. 1A), 38 overlapping upregulated and 103 overlapping downregulated LMRGs in the colorectal carcinoma compared with the normal mucosa (Fig. 1B), and 13 overlapping upregulated and 16 overlapping downregulated LMRGs in the colorectal carcinoma compared with the colorectal adenoma (Fig. 1C), were identified. In total, 149 unique LMRGs were identified (Sheet 1), which reflected the serious lipid metabolism disorders in colorectal tumors. The enriched GO and KEGG analyses suggested that the 149 LMRGs constituted the lipid component of cells, performed the molecular function of

lipid metabolism, participated in the biological process of fatty acid metabolism, and affected a wide range of lipid metabolic pathways (Fig. 1D and E).

The LMRG signature reveals a progressive loss of immune infiltration in colorectal adenoma

The expression of the 149 LMRGs was defined as an LMRG signature. Based on the LMRG signature, the colorectal adenoma samples from the GSE41657 dataset were divided into three clusters (A1, A2, and A3) (Fig. 2A). Gene set variation analysis suggested that most of the 28 immune cells were reduced in the adenoma samples compared with the normal samples (Fig. 2B). Type 1 T helper cells, myeloid-derived suppressor cells (MDSCs), effector memory CD8 T cells, plasmacytoid dendritic cells, CD56 dim natural killer cells, active dendritic cells, and activated CD8 T cells showed a sequential decreasing trend in the three clusters (Fig. 2C). The ESTIMATE algorithm showed a stepwise decreasing trend in the stromal, immune, and ESTIMATE scores in the three sequential clusters (Fig. 2D–F), which suggested gradually reduced immune infiltration and a gradually colder microenvironment in the three sequential clusters. In particular, adenoma with high-grade dysplasia accounted for 21.1% of the samples in cluster A1 but accounted for 90.9% of the samples in cluster A3 (Fig. 2G), which indicated that the three sequential clusters represented the progression of colorectal adenoma. Therefore, the three sequential clusters determined by the LMRG signature revealed a progressive loss of immune infiltration and a stepwise establishment of a cold microenvironment in colorectal adenoma (Fig. 2H).

The LMRG signature reveals a progressive gain of immune infiltration in colorectal adenocarcinoma

A total of 429 colon carcinoma from the TCGA-COAD cohort were grouped into three clusters (C1, C2, and C3) (Fig. 3A). Substantially greater immune infiltration was found in cluster C3 (Fig. 3B). The stromal, immune, and ESTIMATE scores showed gradual gains in these three clusters (Fig. 3C–E). In addition, gradually increased dysfunction scores, exclusion scores, and TIDE scores were observed in the three sequential clusters (Fig. 3F–H). Therefore, the sequential clusters C1, C2, and C3 manifested a progressive gain of immune infiltration with a gradually hot microenvironment and a progressively increased risk of antitumor immune escape. Antitumor immunity can be divided into three types: the immune-desert phenotype, inflamed phenotype, and immune-excluded phenotype [26]. Cluster C1 represented the immune-desert phenotype with no immunotherapeutic response because of an absolute lack of immune cells. Cluster C2 represented the inflamed phenotype that was amenable to immunotherapy because of numerous

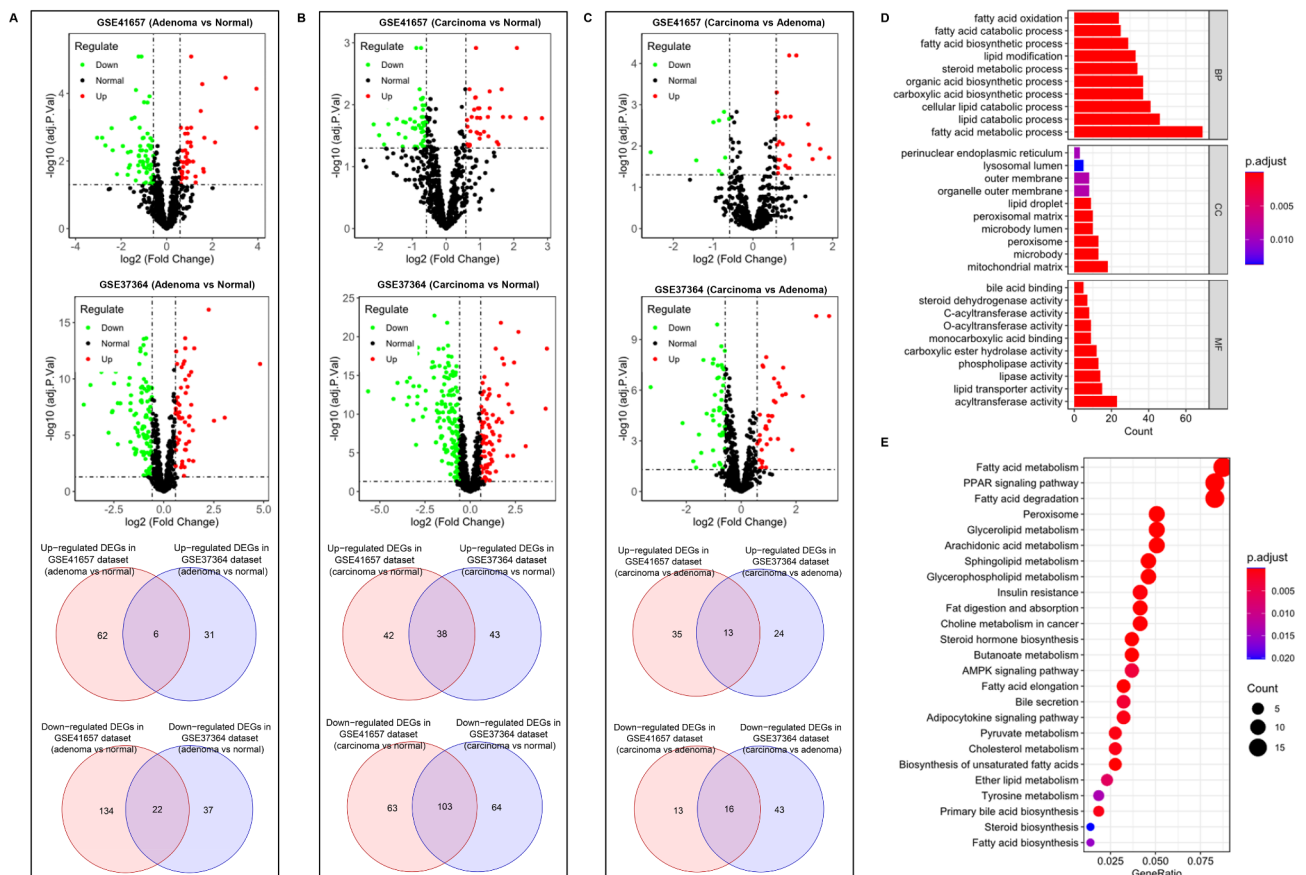


Fig. 1 Identification of differentially expressed LMRGs. The volcano plots show the gene expression regulation in the GSE41657 and GSE37364 datasets. The overlapping upregulated and downregulated genes in the two datasets were intersected by Venn diagrams. **A:** Differentially expressed LMRGs in adenoma samples compared with normal samples. **B:** Differentially expressed LMRGs in carcinoma samples compared with normal samples. **C:** Differentially expressed LMRGs in carcinoma samples compared with adenoma samples. **D:** The Gene Ontology (GO) enrichment terms showed the biological process (BP), cellular component (CC), and molecular function (MF) of 149 differentially expressed LMRGs. **E:** KEGG pathways of 149 differentially expressed LMRGs.

activated and semiactivated immune cells in the tumor microenvironment. Cluster C3 represented the immune-excluded phenotype that had poor effectiveness in immunotherapy because of the inhibition of abundant stromal elements [26]. No obvious differences were observed between the three clusters and TNM stage (Fig. 3I). However, cluster C1 exhibited the best prognosis, and cluster C3 showed the worst prognosis (Fig. 3J), as suggested by the K–M survival curve (log-rank $P=0.011$). As such, the three sequential clusters reflected the progressive development of colorectal carcinoma. The above results suggested that the three sequential clusters determined by the LMRG signature were associated with increased immune infiltration, increased antitumor immune escape, and reduced overall survival in colorectal carcinoma (Fig. 3K), which was opposite to the change in the tumor microenvironment in colorectal adenocarcinoma.

The LMRG signature reveals dynamic immune infiltration along the ACS

The GSE117606 dataset was used to further confirm the above results. As before, both adenoma samples and carcinoma samples were grouped into three clusters (Fig. 4A and B). The relative positions of normal, adenoma, and carcinoma samples exactly represented the course from normal mucosa to adenoma to carcinoma as suggested by the t-SNE analysis (Fig. 4C). Unexpectedly, the sequential clusters of colorectal adenoma and carcinoma showed a directional relationship and collectively constituted the progressive course of colorectal ACS (Fig. 4D). In addition, the stromal, immune, and ESTIMATE scores decreased from cluster A1 to their lowest points in cluster A3 and then gradually rose to their highest points in cluster C3 (Fig. 4E). The infiltration of most immune cells in these clusters also maintained almost the same trend (Fig. 4F). Furthermore, the expression of CD3G (T-cell marker), CD8A (CD8⁺ T-cell marker), CD19 (B-cell marker), and PD-L1 (an immunotherapy target of CRC) maintained the same trend as immune infiltration

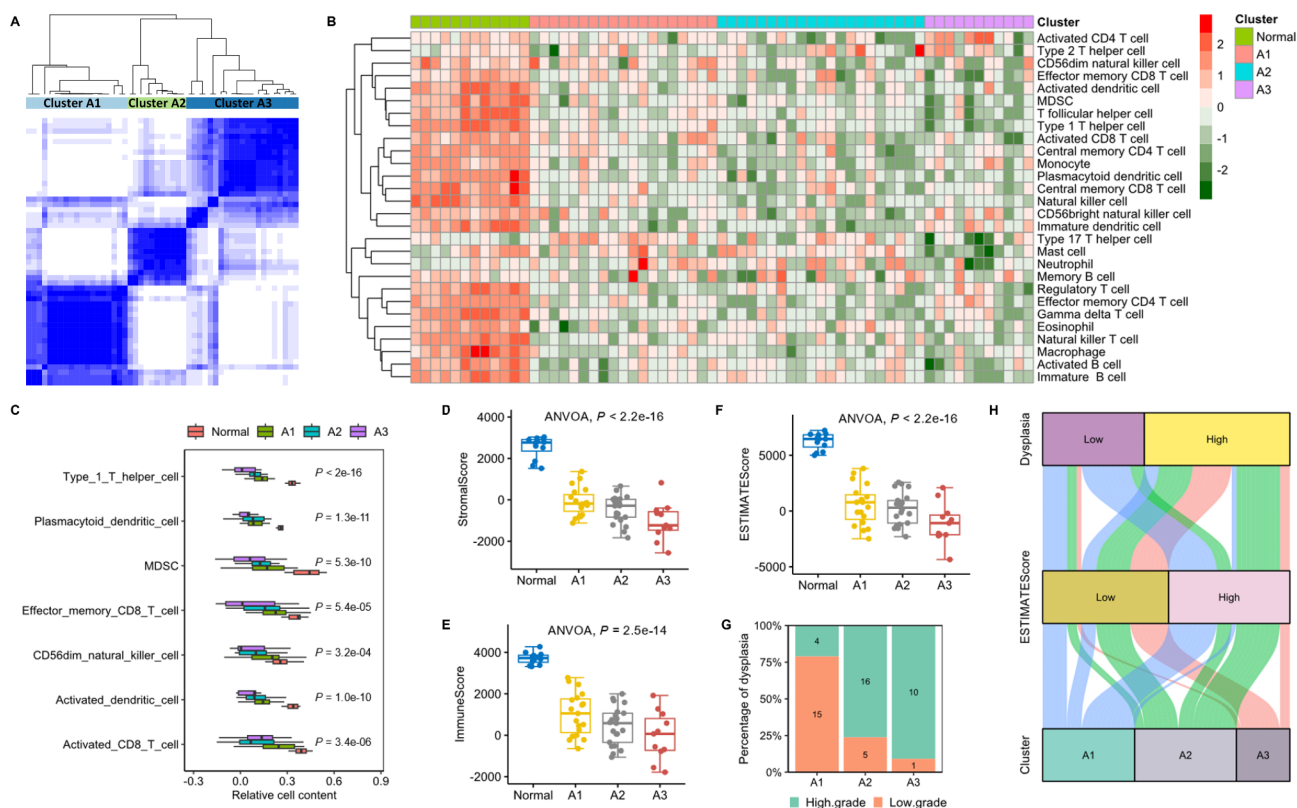


Fig. 2 The LMRG signature revealed a progressive loss of immune infiltration in colorectal adenoma in the GSE41657 dataset. **A:** Consensus clustering of colorectal adenoma samples. **B:** Various immune cell infiltrations in each cluster. **C:** Seven immune cells showed a gradually decreasing trend in the three clusters. **D-F:** Stromal score, immune score, and ESTIMATE score calculated by the ESTIMATE algorithm. **G:** Proportion of samples with low- and high-grade dysplasia in each cluster. **H:** Sankey plot summarizing the relationships among clusters, ESTIMATE score, and dysplasia. ANOVA: analysis of variance

among these clusters (Figure S1A-D). Eight LMRGs (CEBPB, ADH1B, PI3KCG, GLIPR1, CD36, CAV1, G0S2, and PTGS2) were also correlated with the characteristic immune infiltration along the colorectal ACS (Figure S1E-L). The above evidence strongly demonstrated the rationality of analyzing the colorectal ACS based on the LMRG signature, and the LMRG signature revealed that adenoma progression was accompanied by a progressive loss of immune infiltration and a stepwise establishment of a cold microenvironment, but carcinoma progression was characterized by a progressive gain of immune infiltration and a stepwise establishment of a hot microenvironment.

Discussion

In this study, the expression of 149 differentially expressed LMRGs was defined as the LMRG signature. Based on the LMRG signature, the adenoma and carcinoma samples were divided into three clusters. Unexpectedly, these sequential clusters showed a directional relationship and collectively constituted the progressive course of colorectal ACS. Interestingly, the LMRG signature revealed that adenoma progression was accompanied by a progressive loss of immune infiltration and a

stepwise establishment of a cold microenvironment, but carcinoma progression was characterized by a progressive gain of immune infiltration and a gradual establishment of a hot microenvironment (Figure S2).

The ACS is responsible for 85–90% of sporadic CRC cases [27, 28], but it is a very slow process that takes approximately 10–20 years from a normal state to adenoma to cancer diagnosis. During this long course, a high-fat diet is the predominant environmental factor. Although a high-fat diet has been reported to be associated with many cancers, a high-fat diet is a particularly relevant risk factor in CRC and is associated with nearly 80% of CRC cases [6]. Therefore, understanding the role of lipid metabolism in CRC carcinogenesis is highly important. In the current study, 149 differentially expressed LMRGs were identified in colorectal adenoma and carcinoma, which reflects a serous lipid metabolism disorder in colorectal tumors. The clusters determined by the LMRG signature show a directional relationship and collectively constitute the progressive course of colorectal ACS. Perhaps most interestingly, the LMRG signature revealed a dynamic immune infiltration characteristic along the colorectal ACS. The above results reveal the

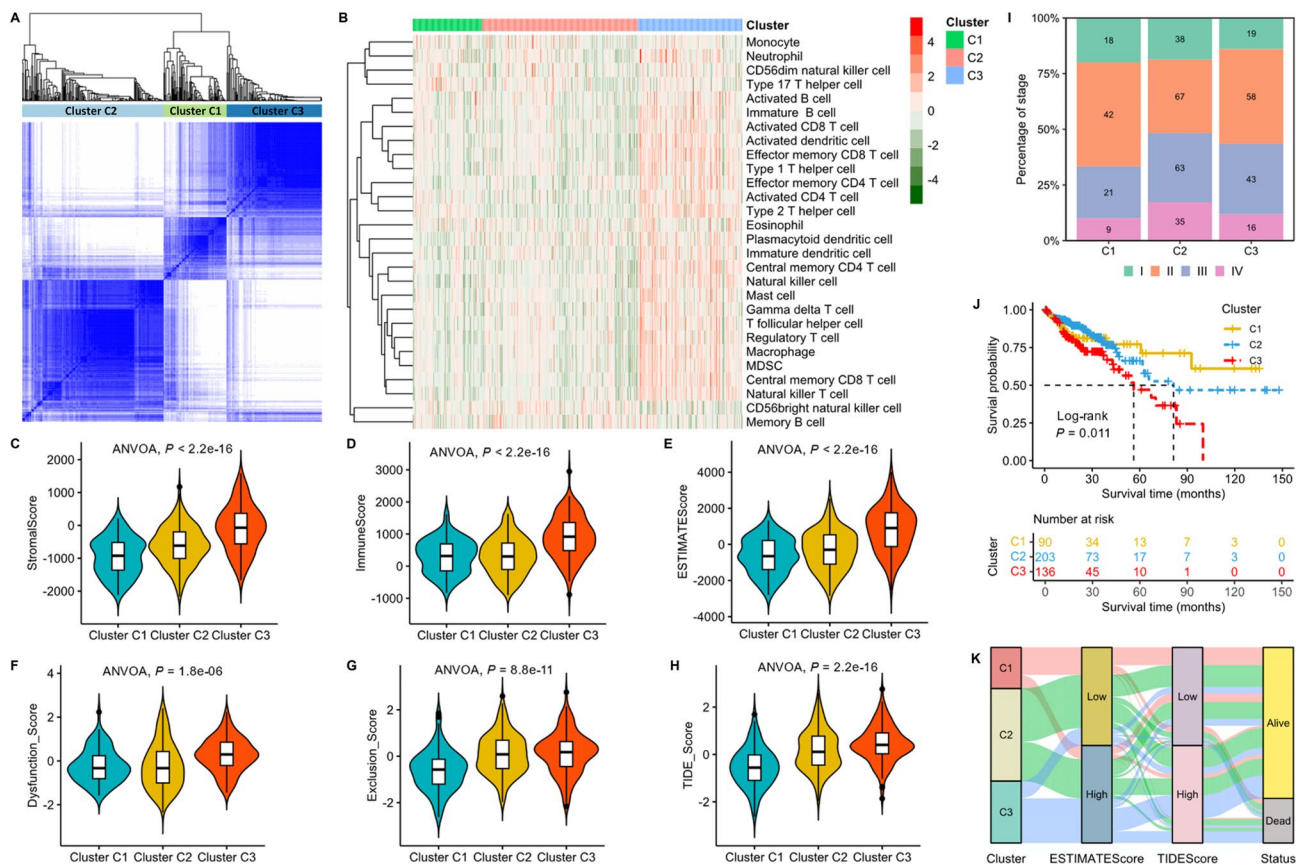


Fig. 3 The LMRG signature reveals a progressive gain of immune infiltration in colorectal adenocarcinoma in the TCGA-COAD cohort. **A:** Consensus clustering analysis of colorectal adenocarcinoma samples. **B:** Various immune cell infiltrations in each cluster. **C–E:** Stroma score, immune score, and ESTIMATE score calculated by the ESTIMATE algorithm. **F–H:** Dysfunction score, exclusion score, and TIDE score in each cluster. **I:** Proportion of various TNM stages in each cluster. **J:** K–M survival curves of each cluster. **K:** Sankey plot summarizing the relationships among clusters, ESTIMATE score, TIDE score and survival status. ANOVA: analysis of variance

important role of lipid metabolism in the tumor microenvironment of CRC.

Fatty acid oxidation can promote the effects of PD-1 antibody in CD8⁺ T cells and enhance the survival of CD8⁺ tissue-resident memory T cells, but excessive fatty acid oxidation inhibits the antitumor ability of effector T cells and supports the immunosuppressive function of regulatory T cells in the tumor microenvironment [29]. Thus, lipid metabolic alterations are closely related to the functional status of immune cells. A few studies have reported that LMRGs are immune-related prognostic indicators in various cancers, and many LMRG signatures have been constructed to evaluate the tumor microenvironment and identify different immune clusters [10, 11, 30, 31]. Unlike previous studies, the current study did not emphasize the role of specific LMRGs but instead constructed clusters of colorectal tumors based on the LMRG signature. Surprisingly, evidence suggested that these clusters showed a directional relationship and collectively constituted the progressive course of colorectal ACS. In addition, this study did not focus solely on the

clusters of carcinoma samples but rather on the complete process of colorectal ACS. Consequently, the current study revealed dynamic immune infiltration along the colorectal ACS based on the LMRG signature.

A previous study reported that tumor infiltration based on immune cell counts decreased in adenomas with low-grade dysplasia, adenomas with high-grade dysplasia, and invasive adenocarcinomas according to a small number of adenoma and carcinoma samples [32]; these findings share some similarities with those of the current research. However, the current study found that as adenomas undergo cancerous transformation, carcinoma progression is characterized by a progressive gain of immune infiltration. In fact, several studies have revealed the immune subtypes in COAD [33–35], and the immune subtypes in these studies also share similarity with the current research. However, they did not find a connection between different clusters. Unfortunately, there is no relevant research to elucidate the molecular mechanism by which immune infiltration in colorectal adenomas and carcinomas changes in this way. The progressive loss

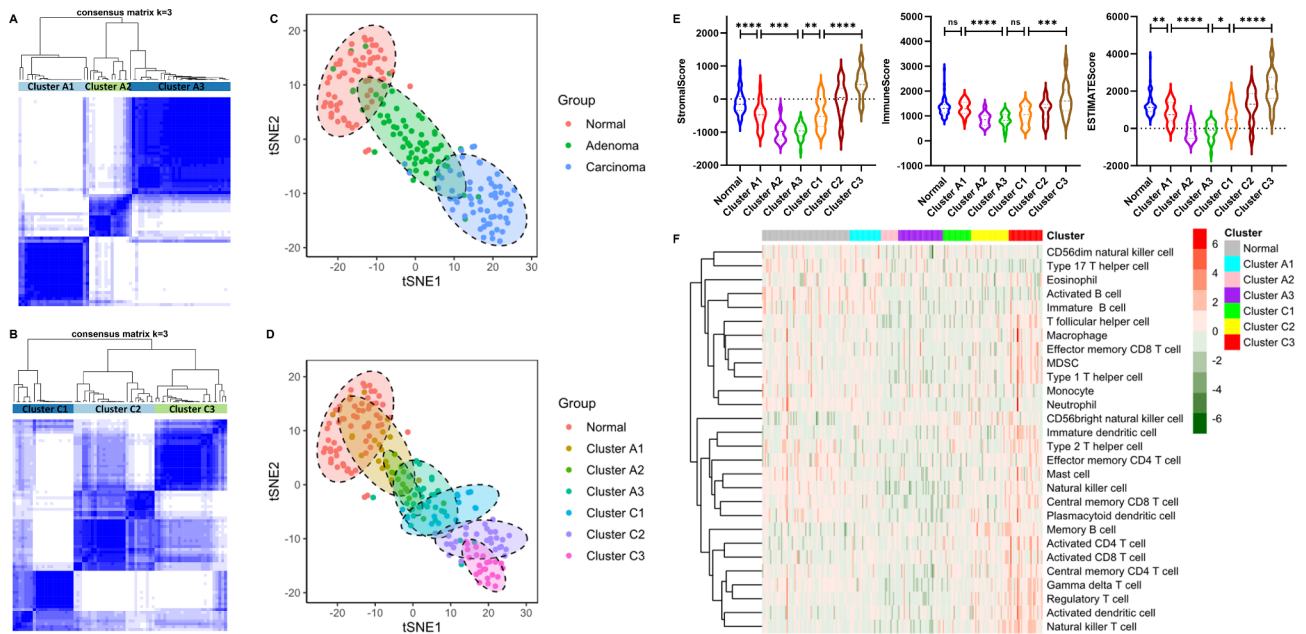


Fig. 4 The LMRG signature reveals dynamic immune infiltration across the ACS in the GSE117606 dataset. **A** and **B**: Consensus clustering analysis of colorectal adenoma and carcinoma samples. **C**: t-SNE plot of three different colorectal samples. **D**: t-SNE plot of each cluster. **E**: Stromal score, immune score, and ESTIMATE score for each cluster. **F**: Various immune cell infiltrations in each cluster. ns: not significant; *, $P < 0.05$; **, $P < 0.01$; ***, $P < 0.001$; ****, $P < 0.0001$

of immune infiltration in colorectal adenoma suggests a morbid exhaustion of immune cells that likely results from persistent antigen stimulation and chronic inflammation, and the progressive gain of immune infiltration in CRC suggests a diseased activation of immune cells that may be attributed to the secondary response of the body's antitumor immunity.

Immune cells can be divided into immune promoting related cells (CD8 T cells, monocytes, dendritic cells, etc.) that are associated with good clinical outcomes and immunosuppressive related cells (MDSCs and regulatory T cells) that are associated with poor clinical outcomes. We found that there was a consistent trend in the infiltration level of immune promoting related cells and immune suppressing related cells along the ACS. The MDSCs, regulatory T cells, and most of the immune promoting related cells showed reduced trend with the progressive development of colorectal adenoma, which suggests a morbid exhaustion of immune cells that likely results from persistent antigen stimulation and chronic inflammation. The more immune cells are exhausted, the worse the pathological type of the patient. On contrary, these cells exhibited increased trend with the development of colorectal carcinoma, which suggests a diseased activation of immune cells that may be attributed to the secondary response of the body's antitumor immunity. The cluster C3 that had the most abundant immune infiltration but the highest risk of immune escape and the worst prognosis may be related to the significantly increased

immune infiltration of immunosuppressive related cells. These viewpoints suggested that the immunosuppressive related cells may have a greater effect on inhibiting the activity of other immune cells than reducing their counts, and a certain immune cell alone could not be reliable to determine the immune status and prognosis of tumor patients as the functional states of different immune cells can interact with each other. Therefore, a comprehensive understanding of the immune infiltration in the tumor microenvironment is vital for evaluating the immune status and prognosis of patients with colorectal neoplasm.

Study strength and limitations

This study reveals dynamic immune infiltration along the colorectal ACS, which substantially changes the understanding of the tumor microenvironment of CRC. The major limitation of this study is that all gene expression data were obtained from public databases and lack experimental validation in vivo and in vitro, as well as the unavailability of histological evidence. However, similar results were obtained from different algorithms and multiple cohorts, which improves the accuracy and stability of the conclusions. Nevertheless, further experiments are necessary.

Conclusions

In summary, the LMRG signature reveals that adenoma progression is accompanied by a progressive loss of immune infiltration and a stepwise establishment of a

cold microenvironment, but carcinoma progression is characterized by a progressive gain of immune infiltration and a gradual establishment of a hot microenvironment. The progressive loss of immune infiltration in colorectal adenoma suggests a morbid exhaustion of immune cells that likely results from persistent antigen stimulation and chronic inflammation, and the progressive gain of immune infiltration in colorectal carcinoma suggests a diseased activation of immune cells that may be attributed to the secondary response of the body's antitumor immunity. These findings substantially change the understanding of the tumor microenvironment of CRC and provide novel insight into the role of lipid metabolism in this process.

Abbreviations

CRC	Colorectal cancer
ACS	Adenoma-carcinoma sequence
LMRGs	Lipid metabolism-related genes
GEO	Gene Expression Omnibus
TCGA	The Cancer Genome Atlas
COAD	Colon adenocarcinoma
t-SNE	t-distributed stochastic neighbor embedding
KEGG	Kyoto Encyclopedia of Genes and Genomes
GO	Gene Ontology
TIDE	Tumor Immune Dysfunction and Exclusion
K-M	Kaplan-Meier
BP	Biological process
CC	Cellular component
MF	Molecular function

Supplementary Information

The online version contains supplementary material available at <https://doi.org/10.1186/s12944-023-01866-4>.

Supplementary Material 1
Supplementary Material 2
Supplementary Material 3
Supplementary Material 4

Acknowledgements

We are grateful to the contributors to the public databases used in this study.

Authors' contributions

All authors contributed to the study conception and design. Material preparation, data collection and analysis were performed by Jie Chen and Jianfang Ye. Jie Chen performed the statistical analyses and wrote the first draft. Jianfang Ye revised the manuscript. Renxu Lai oversaw the project and provided the funding source. All authors commented on previous versions of the manuscript and approved the final manuscript.

Funding

Not applicable.

Data Availability

All participants were identified through public GEO and TCGA databases. The datasets supporting the conclusions of this article are included within the additional file.

Declarations

Competing interests

The authors declare no competing interests.

Ethics approval and consent to participate

Not applicable.

Consent for publication

Not applicable.

Received: 28 March 2023 / Accepted: 29 June 2023

Published online: 04 July 2023

References

1. Sung H, Ferlay J, Siegel RL, Laversanne M, Soerjomataram I, Jemal A, Bray F. Global Cancer Statistics 2020: GLOBOCAN estimates of incidence and Mortality Worldwide for 36 cancers in 185 countries. *CA Cancer J Clin.* 2021;71:209–49. <https://doi.org/10.3322/caac.21660>.
2. Gonzalez-Gonzalez M, Gutierrez ML, Sayagues JM, Munoz-Bellvis L, Orfao A. Genomic profiling of sporadic liver metastatic colorectal cancer. *Semin Cancer Biol.* 2021;71:98–108. <https://doi.org/10.1016/j.semcancer.2020.05.013>.
3. Keum N, Giovannucci E. Global burden of colorectal cancer: emerging trends, risk factors and prevention strategies. *Nat Rev Gastroenterol Hepatol.* 2019;16:713–32. <https://doi.org/10.1038/s41575-019-0189-8>.
4. Bian X, Liu R, Meng Y, Xing D, Xu D, Lu Z. Lipid metabolism and cancer. *J Exp Med* 2021; 218. <https://doi.org/10.1084/jem.20201606>.
5. Broadfield LA, Pane AA, Talebi A, Swinnen JV, Fendt SM. Lipid metabolism in cancer: new perspectives and emerging mechanisms. *Dev Cell.* 2021;56:1363–93. <https://doi.org/10.1016/j.devcel.2021.04.013>.
6. Karunanithi S, Levi L, DeVecchio J, Karagkounis G, Reizes O, Lathia JD, Kalady MF, Noy N. RBP4-STRA6 pathway drives Cancer Stem Cell maintenance and mediates High-Fat Diet-Induced Colon carcinogenesis. *Stem Cell Reports.* 2017;9:438–50. <https://doi.org/10.1016/j.stemcr.2017.06.002>.
7. Zhu QC, Gao RY, Wu W, Guo BM, Peng JY, Qin HL. Effect of a high-fat diet in development of colonic adenoma in an animal model. *World J Gastroenterol.* 2014;20:8119–29. <https://doi.org/10.3748/wjg.v20.i25.8119>.
8. Wang D, Fu L, Wei J, Xiong Y, DuBois RN. PPARdelta mediates the Effect of Dietary Fat in promoting Colorectal Cancer Metastasis. *Cancer Res.* 2019;79:4480–90. <https://doi.org/10.1158/0008-5472.CAN-19-0384>.
9. Zhang A, Miao K, Sun H, Deng CX. Tumor heterogeneity reshapes the tumor microenvironment to influence drug resistance. *Int J Biol Sci.* 2022;18:3019–33. <https://doi.org/10.7150/ijbs.72534>.
10. Yang C, Huang S, Cao F, Zheng Y. A lipid metabolism-related genes prognosis biomarker associated with the tumor immune microenvironment in colorectal carcinoma. *BMC Cancer.* 2021;21:1182. <https://doi.org/10.1186/s12885-021-08902-5>.
11. Lin D, Fan W, Zhang R, Zhao E, Li P, Zhou W, Peng J, Li L. Molecular subtype identification and prognosis stratification by a metabolism-related gene expression signature in colorectal cancer. *J Transl Med.* 2021;19:279. <https://doi.org/10.1186/s12967-021-02952-w>.
12. Huang Y, Zhou J, Zhong H, Xie N, Zhang FR, Zhang Z. Identification of a novel lipid metabolism-related gene signature for predicting colorectal cancer survival. *Front Genet.* 2022;13:989327. <https://doi.org/10.3389/fgene.2022.989327>.
13. Liberzon A, Subramanian A, Pinchback R, Thorvaldsdottir H, Tamayo P, Mesirov JP. Molecular signatures database (MSigDB) 3.0. *Bioinformatics.* 2011;27:1739–40. <https://doi.org/10.1093/bioinformatics/btr260>.
14. Sun X, Zhang Y, Chen Y, Xin S, Jin L, Liu X, Zhou Z, Zhang J, Mei W, Zhang B, Yao X, Yang G, Ye L. In Silico Establishment and Validation of Novel Lipid Metabolism-Related Gene Signature in Bladder Cancer. *Oxid Med Cell Longev* 2022; 2022:3170950. <https://doi.org/10.1155/2022/3170950>.
15. Ritchie ME, Phipson B, Wu D, Hu Y, Law CW, Shi W, Smyth GK. Limma powers differential expression analyses for RNA-sequencing and microarray studies. *Nucleic Acids Res.* 2015;43:e47. <https://doi.org/10.1093/nar/gkv007>.
16. Yu G, Wang LG, Han Y, He QY. clusterProfiler: an R package for comparing biological themes among gene clusters. *OMICS.* 2012;16:284–7. <https://doi.org/10.1089/omi.2011.0118>.
17. Liu J, Chen C, Wang Y, Qian C, Wei J, Xing Y, Bai J. Comprehensive of N1-Methyladenosine modifications patterns and immunological characteristics in Ovarian Cancer. *Front Immunol.* 2021;12:746647. <https://doi.org/10.3389/fimmu.2021.746647>.

18. Liu J, Wang Y, Yuan S, Wei J, Bai J. Construction of an Immune cell infiltration score to evaluate the prognosis and therapeutic efficacy of Ovarian Cancer Patients. *Front Immunol*. 2021;12:751594. <https://doi.org/10.3389/fimmu.2021.751594>.
19. Liu J, Geng R, Ni S, Cai L, Yang S, Shao F, Bai J. Pyroptosis-related lncRNAs are potential biomarkers for predicting prognoses and immune responses in patients with UCEC. *Mol Ther Nucleic Acids*. 2022;27:1036–55. <https://doi.org/10.1016/j.omtn.2022.01.018>.
20. Wilkerson MD, Hayes DN. ConsensusClusterPlus: a class discovery tool with confidence assessments and item tracking. *Bioinformatics*. 2010;26:1572–3. <https://doi.org/10.1093/bioinformatics/btq170>.
21. Cheng Y, Wang X, Xia Y. Supervised t-distributed stochastic neighbor embedding for data visualization and classification. *INFORMS J Comput*. 2021;33:419–835. <https://doi.org/10.1287/ijoc.2020.0961>.
22. Yoshihara K, Shahmoradgoli M, Martinez E, Vegesna R, Kim H, Torres-Garcia W, Trevino V, Shen H, Laird PW, Levine DA, Carter SL, Getz G, Stemke-Hale K, Mills GB, Verhaak RG. Inferring tumour purity and stromal and immune cell admixture from expression data. *Nat Commun*. 2013;4:2612. <https://doi.org/10.1038/ncomms3612>.
23. Charoentong P, Finotello F, Angelova M, Mayer C, Efremova M, Rieder D, Hackl H, Trajanoski Z. Pan-cancer immunogenomic analyses reveal genotype-immunophenotype Relationships and Predictors of response to checkpoint blockade. *Cell Rep*. 2017;18:248–62. <https://doi.org/10.1016/j.celrep.2016.12.019>.
24. Jiang P, Gu S, Pan D, Fu J, Sahu A, Hu X, Li Z, Traugh N, Bu X, Li B, Liu J, Freeman GJ, Brown MA, Wucherpfennig KW, Liu XS. Signatures of T cell dysfunction and exclusion predict cancer immunotherapy response. *Nat Med*. 2018;24:1550–8. <https://doi.org/10.1038/s41591-018-0136-1>.
25. Brunson JC. ggalluvial: layered grammar for alluvial plots. *J Open Source Softw*. 2020;5. <https://doi.org/10.21105/joss.02017>.
26. Chen DS, Mellman I. Elements of cancer immunity and the cancer-immune set point. *Nature*. 2017;541:321–30. <https://doi.org/10.1038/nature21349>.
27. Fearon ER, Vogelstein B. A genetic model for colorectal tumorigenesis. *Cell*. 1990;61:759–67. [https://doi.org/10.1016/0092-8674\(90\)90186-i](https://doi.org/10.1016/0092-8674(90)90186-i).
28. Cancer Genome Atlas N. Comprehensive molecular characterization of human colon and rectal cancer. *Nature*. 2012;487:330–7. <https://doi.org/10.1038/nature11252>.
29. Yu W, Lei Q, Yang L, Qin G, Liu S, Wang D, Ping Y, Zhang Y. Contradictory roles of lipid metabolism in immune response within the tumor micro-environment. *J Hemato Oncol*. 2021;14:187. <https://doi.org/10.1186/s13045-021-01200-4>.
30. Yang S, Sun B, Li W, Yang H, Li N, Zhang X. Fatty acid metabolism is related to the immune microenvironment changes of gastric cancer and RGS2 is a new tumor biomarker. *Front Immunol*. 2022;13:1065927. <https://doi.org/10.3389/fimmu.2022.1065927>.
31. Zhang Y, Kong X, Xin S, Bi L, Sun X. Discovery of lipid metabolism-related genes for Predicting Tumor Immune Microenvironment Status and prognosis in prostate Cancer. *J Oncol*. 2022;2022:8227806. <https://doi.org/10.1155/2022/8227806>.
32. Freitas JA, Gullo I, Garcia D, Miranda S, Spaans L, Pinho L, Reis J, Sousa F, Baptista M, Resende C, Leitao D, Duraes C, Costa JL, Carneiro F, Machado JC. The adaptive Immune Landscape of the colorectal adenoma-carcinoma sequence. *Int J Mol Sci*. 2021;22. <https://doi.org/10.3390/ijms22189791>.
33. Chen Y, Zhao J. Identification of an Immune Gene signature based on Tumor Microenvironment characteristics in Colon adenocarcinoma. *Cell Transpl*. 2021;30:9636897211001314. <https://doi.org/10.1177/09636897211001314>.
34. Qi W, Zhang Q. Identification and validation of Immune Molecular Subtypes and Immune Landscape based on Colon cancer cohort. *Front Med (Lausanne)*. 2022;9:827695. <https://doi.org/10.3389/fmed.2022.827695>.
35. Qiu C, Shi W, Wu H, Zou S, Li J, Wang D, Liu G, Song Z, Xu X, Hu J, Geng H. Identification of Molecular Subtypes and a prognostic signature based on inflammation-related genes in Colon adenocarcinoma. *Front Immunol*. 2021;12:769685. <https://doi.org/10.3389/fimmu.2021.769685>.

Publisher's Note

Springer Nature remains neutral with regard to jurisdictional claims in published maps and institutional affiliations.